

Phase structures of neutral dense quark matter and application to strange quark stars

Shu-Sheng Xu,^{a,1}

^a*School of Science, Nanjing University of Posts and Telecommunications, Nanjing 210023, China*

E-mail: xuss@njupt.edu.cn

ABSTRACT: In the contact interaction model, the quark propagator has only one solution, chiral symmetry breaking solution, at vanish temperature and density. Inspire by Y. Jiang and Z.-F. Cui [1, 2], we introduce 2+1 flavors quark condensates feedback on coupling strength, the Wigner solution appears in some region of parameters. It enables us to tackle chiral phase transition as two-phase coexistences. At finite chemical potential, we analyze the chiral phase transition to the conditions of electric charge neutrality and β equilibrium. The four chemical potentials, μ_u , μ_d , μ_s and μ_e , are constrained by three conditions, there is one independent variable that remained, we choose the average quark chemical potential as the free variable. All quark masses and number densities suffer discontinuities at the phase transition point. The strange quarks appear after the phase transition due to the system needs more energy to produce a d-quark than an s-quark. Take the EOS as an input, the TOV equations are solved numerically, we show that the mass-radius relation is sensitive to the EOSs. The maximum mass of strange quark stars is not susceptible to our introduced parameter Λ_q .

¹Corresponding author.

Contents

1	Introduction	1
2	Quark propagators in vacuum	2
3	The chiral phase structure in neutral dense quark matter	5
4	Application to strange quark stars	7
5	Summary	8

1 Introduction

It is well-known that hadrons with strangeness are unstable, they could decay into lighter hadrons made of non-strange quarks through the weak interaction. The hypothesis of stable strange nuclei is first proposed by A. Bodmer in Ref. [3]. Afterward, E. Witten proposed stable dense quark matter containing strange quarks based on the assumption that the Fermi momentum of the system exceeds the strange quark mass in the dense quark matter, therefore the dense quark matter favors some non-strange quarks transform into strange quarks [4]. There are plenty of studies on strange quark stars from that time on [5–11]. Especially, after the gravitational waves are detected from the merging of compact stars, people are interested in exploring the inner structure of compact stars [12–15].

The properties of dense QCD play a key role in the structure of compact stars, but lattice regularized QCD can not deal with such systems since the technical difficulty, that is “sign problem”. Various effective models are inevitably used to study the phase structures of dense QCD systems, such as the quasi-particle model [16–22], quark-meson model [23–28], Nambu-Jona-Lasinio (NJL) model [2, 29–35], and some effective models of Dyson-Schwinger equations (DSEs) [36–48]. Based on these model studies, people believed that there are colorful phase structures in dense QCD matter. Most of these model studies find there is a critical endpoint (CEP) in the phase diagram. The chiral phase transition happens at low temperature and high density, while the low density and high-temperature region is crossover. In terms of cold dense QCD, DSEs confront a difficulty that the quark propagator has poles at high baryon chemical potential. NJL model also has a drawback that there is an only one solution, and the pressure of the system is discontinuous at the chiral phase transition point, therefore the EOS is incomplete. In order to resolve this problem, the quark condensates feedback approach is proposed in the contact interaction model [1, 2]. In this approach, the coupling strength depends on the quark condensates, and the Wigner solution appears for some parameter choice.

In this work, we will borrow this idea and extend it to 2+1 flavors to study dense QCD phase structure and strange quark stars. This paper is organized as follows. We

give a basic introduction to the quark gap equation and the quark condensate feedback approach in the 2+1 flavor case in Sec. 2, the solutions of the quark propagator are shown and related parameters are fixed by pion and kaon observables. In Sec. 3, the dense QCD phase structures are studied in conditions of electric charge neutrality and β equilibrium. The EOS as an input, the mass-radius relation is given in Sec. 4. And finally, we summarize our studies in Sec. 5.

2 Quark propagators in vacuum

The quark propagator plays a central role in many issues, it satisfies the Dyson-Schwinger equation,

$$S_f^{-1}(p) = S_{f0}^{-1}(p) + g^2 \int \frac{d^4 q}{(2\pi)^4} D_{\mu\nu}(p-q) \gamma_\mu t^a S_f(p) \Gamma_\nu^a(p, q). \quad (2.1)$$

where $S_{f0}(p)$ is the bare quark propagator with flavor f , $S_f(p)$ is the dressed quark propagator, $\Gamma_\nu^a(p, q)$ is the amputated quark-gluon vertex, $D_{\mu\nu}(p-q)$ is the dressed gluon propagator. It is the exact equation, which derived from QCD generating functional. The quark propagator (two-point Green function) is related to the quark-gluon vertex (three-point Green function), and the three-point Green function is related to higher-point Green functions. They are infinitely coupled integral equations. Thus, specific truncation for DSEs is necessary. Rainbow truncation is simple and preserves chiral symmetry,

$$\Gamma_\nu^a(p, q) \longrightarrow \gamma_\nu t^a, \quad (2.2)$$

which is widely used in hadron physics and thermal and dense QCD. The quark DSE is closed if dressed gluon propagator is specified. We use the contact interaction model in this work [49], that is

$$g^2 D_{\mu\nu}(p-q) = \frac{1}{M_G^2} \delta_{\mu\nu}. \quad (2.3)$$

The quark DSE turns to

$$S_f^{-1}(p) = S_{f0}^{-1}(p) + \frac{4}{3M_G^2} \int^\Lambda \frac{d^4 q}{(2\pi)^4} \gamma_\mu S_f(p) \gamma_\mu. \quad (2.4)$$

The integration in Eq. (2.4) with this model is divergent, the 3-dimension cut-off is performed in this work [50]. The inverse of quark propagator have the general structure

$$S_f^{-1}(p) = i\gamma \cdot p A_f(p^2) + B_f(p^2), \quad (2.5)$$

where $A_f(p^2)$ and $B_f(p^2)$ are two scalar functions. Substituting Eqs. (2.2), (2.3) and (2.5) into Eq. (2.1), one can obtain $A_f(p^2) = 1$, $B_f(p^2) = M_f$ is a constant mass, which satisfies

$$\begin{aligned} M_f &= m_f + \frac{4}{3M_G^2} \int^\Lambda \text{Tr}_D[S_f(p)] \\ &= m_f + \frac{4}{3M_G^2} \int^\Lambda \frac{d^4 q}{(2\pi)^4} \frac{4M_f}{q^2 + M_f^2} \\ &= m_f + \frac{2M_f}{3M_G^2 \pi^2} \left[\Lambda \sqrt{\Lambda^2 + M_f^2} - M_f^2 \ln \left(\frac{\Lambda}{M_f} + \sqrt{1 + \frac{\Lambda^2}{M_f^2}} \right) \right]. \end{aligned} \quad (2.6)$$

m_u	m_s	M_G	Λ	M_u	M_s	m_π	m_K	f_π	$-\langle\bar{u}u\rangle^{\frac{1}{3}}$	$-\langle\bar{s}s\rangle^{\frac{1}{3}}$
4.3	110	189	799	314.6	547.5	139.3	498.2	93.3	292.2	327.6

Table 1. Model parameters and observables (all quantities in MeV).

There are four parameters in this model, namely $m_u = m_d$, m_s , M_G and Λ , which are fitted by pion mass, pion constant, kaon mass, and light quark condensate [51, 52]. The parameters and corresponding observables are listed in Table. 1. To analysis the solution of quark DSE, it is helpful to define a function

$$F(M_f) = M_f - m_f - \frac{2M_f}{3M_G^2\pi^2}\mathcal{C}(M_f, \Lambda), \quad (2.7)$$

with

$$\mathcal{C}(M_f, \Lambda) = \Lambda\sqrt{\Lambda^2 + M_f^2} - M_f^2 \ln\left(\frac{\Lambda}{M_f} + \sqrt{1 + \frac{\Lambda^2}{M_f^2}}\right). \quad (2.8)$$

One can plot the function $F(M_f)$ for u- and s-quarks, as shown in Fig. 1. We can see that both functions have only one zero points, which implies they are only one solution in a vacuum.

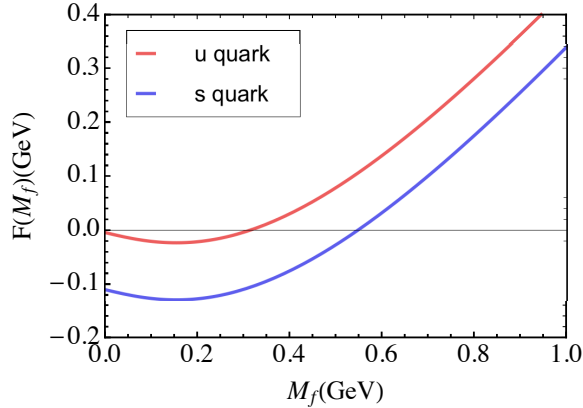


Figure 1. The function $F(M_f)$ for u and s quarks.

According to the gluon DSE, the inverse of gluon propagator includes two parts, namely pure Yang-Mills terms and quark-loop term. The effective interaction between quarks, which relates to the dressed gluon propagator, should depend on the feedback of the quark-loop. Therefore, the effective interaction would be different for different solutions. Inspired from Ref. [1], we use the interaction

$$g^2 D_{\mu\nu}(k) = \delta_{\mu\nu} \frac{1}{M_{\text{eff}}^2} = \delta_{\mu\nu} \left(\frac{1}{M_G'^2} - \sum_{f=u,d,s} \frac{1}{M_G'^2} \frac{\langle\bar{f}f\rangle}{\Lambda_f^3} \right), \quad (2.9)$$

where

$$\langle\bar{f}f\rangle = \frac{N_c M_f}{2\pi^2} \mathcal{C}(M_f, \Lambda). \quad (2.10)$$

Although there are three energy scales Λ_f , we minimize parameters, namely use the same value $\Lambda_u = \Lambda_d = \Lambda_s = \Lambda_q$, in this work. The modified interaction introduces two new parameters, M'_G and Λ_q . We fix $M_{\text{eff}} = M_G$ in the Nambu solution and discuss the dependence of the parameters as the first step. It implies

$$M_G'^2 = M_G^2 \left(1 - \sum_{f=u,d,s} \frac{\langle \bar{f}f \rangle}{\Lambda_q^3} \right). \quad (2.11)$$

The quark DSEs of 3 flavors are coupled to each other, we can define two functions

$$\begin{aligned} F_u(M_u, M_s) &= M_u - m_u - \frac{2M_u}{3M_{\text{eff}}^2 \pi^2} \mathcal{C}(M_u, \Lambda), \\ F_s(M_u, M_s) &= M_s - m_s - \frac{2M_s}{3M_{\text{eff}}^2 \pi^2} \mathcal{C}(M_s, \Lambda). \end{aligned} \quad (2.12)$$

with the $\frac{1}{M_{\text{eff}}^2}$ presented in Eq. (2.9). The solution locates at conditions of $F_u(M_u, M_s) = 0$ and $F_s(M_u, M_s) = 0$. We plot them in Fig. 2, the green curved surface is $F_u(M_u, M_s)$ and the red is $F_s(M_u, M_s)$. We can see that there is only one solution if $\Lambda_q > 0.381$ GeV. When the Λ_q increases to 0.381 GeV, the two solutions happen to appear. The three solutions arise if $\Lambda_q < 0.381$ GeV, but the Λ_q should be restricted between 0.30 GeV and 0.381 GeV if we require the largest mass of the solution is same as the original Nambu solution's mass. Up to now, the model parameters are fixed except Λ_q , we will use $\Lambda_q = 0.38$ GeV to study the properties of neutral dense quark matter in the next section. Thereafter, we will discuss the EOS and mass-radius relation dependence on Λ_q .

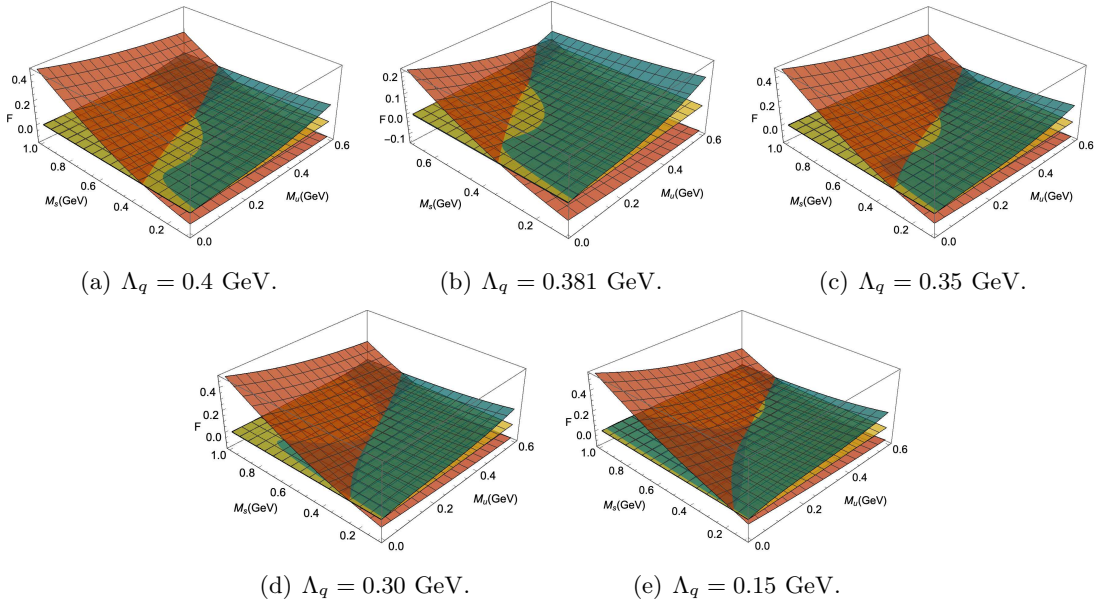


Figure 2. The F_u and F_s as functions of M_u and M_s , the green curved surface is F_u , the red one is F_s , and the yellow one is $F = 0$. The intersections of three surfaces are the solutions of the quark DSEs.

3 The chiral phase structure in neutral dense quark matter

We now turn our attention to the QCD system at finite chemical potentials. The general structure of the inverse of quark propagator is [1]

$$S_f^{-1}(p, \mu_f) = i\gamma \cdot p A_f(p, \mu_f) + B_f(p, \mu_f) - \gamma_4 C_f(p, \mu_f). \quad (3.1)$$

Inserting Eq. (3.1) into Eq. (2.4), one can easily find that $A_f(p, \mu_f) = 1$, $B_f(p, \mu_f) = M_f$, and $C_f(p, \mu_f) = \mu_f^*$ are constant quantities, where M_f and μ_f^* can be regarded as effective mass and chemical potential respectively. They satisfy

$$\begin{aligned} M_f &= m_f + \frac{4}{3M_{\text{eff}}^2} \int^\Lambda \frac{d^4 q}{(2\pi)^4} \frac{4M_f}{q^2 + M_f^2 - \mu_f^{*2} + 2i\mu_f^* q_4} \\ &= m_f + \frac{4}{3M_{\text{eff}}^2} \int^\Lambda \frac{d^3 \vec{q}}{(2\pi)^4} \int_{-\infty}^{\infty} dq_4 \frac{4M_f}{q_4^2 + 2i\mu_f^* q_4 + E_{qMf}^2 - \mu_f^{*2}}, \end{aligned} \quad (3.2)$$

$$\begin{aligned} \mu_f^* &= \mu_f - \frac{4}{3M_{\text{eff}}^2} \int^\Lambda \frac{d^4 q}{(2\pi)^4} \frac{2(iq_4 - \mu_f^*)}{q_4^2 + E_{qMf}^2 - \mu_f^{*2} + 2i\mu_f^* q_4} \\ &= \mu_f - \frac{8}{3M_{\text{eff}}^2} \int^\Lambda \frac{d^3 \vec{q}}{(2\pi)^4} \int_{-\infty}^{\infty} dq_4 \frac{iq_4 - \mu_f^*}{q_4^2 + 2i\mu_f^* q_4 + E_{qMf}^2 - \mu_f^{*2}}, \end{aligned} \quad (3.3)$$

with

$$E_{qMf} = \sqrt{\vec{q}^2 + M_f^2}. \quad (3.4)$$

After some algebraic derivations, one finally obtains

$$M_f = m_f + \frac{2M_f}{3\pi^2 M_{\text{eff}}^2} \mathcal{D}(\mu_f^*, M_f), \quad (3.5)$$

$$\mu_f^* = \mu_f - \frac{2}{3\pi^2 M_{\text{eff}}^2} \left(\mu_f^{*2} - M_f^2 \right)^{3/2} \theta(\mu_f^* - M_f), \quad (3.6)$$

$$\frac{1}{M_{\text{eff}}^2} = \frac{1}{M_G^2} + \sum_{f=u,d,s} \frac{1}{M_G^2 \Lambda_q^3} \frac{N_c M_f}{2\pi^2} \mathcal{D}(\mu_f^*, M_f), \quad (3.7)$$

with

$$\begin{aligned} \mathcal{D}(\mu_f^*, M_f) &= \left[\Lambda \sqrt{\Lambda^2 + M_f^2} - M_f^2 \ln \left(\frac{\Lambda}{M_f} + \sqrt{1 + \frac{\Lambda^2}{M_f^2}} \right) \right] \\ &\quad - \theta(\mu_f^* - M_f) \left[\mu_f^* \sqrt{\mu_f^{*2} - M_f^2} - M_f^2 \ln \left(\frac{\sqrt{\mu_f^{*2} - M_f^2}}{M_f} + \frac{\mu_f^*}{M_f} \right) \right]. \end{aligned} \quad (3.8)$$

There is no difficulty in principle to solve the coupled Eqs. (3.5), (3.6) and (3.7) iteratively, each quantity, such as effective mass, quark number densities, as functions of three different chemical potentials. In this work, we will focus on the phase structures in conditions of electric charge neutrality and β equilibrium. The β equilibrium requires

$$\mu_d = \mu_u + \mu_e, \quad (3.9)$$

$$\mu_s = \mu_d. \quad (3.10)$$

The condition of electric charge neutrality is

$$\frac{2}{3}n_u - \frac{1}{3}n_d - \frac{1}{3}n_s - n_e = 0, \quad (3.11)$$

where n_u, n_d, n_s and n_e are particle number densities for u-, d-, s-quarks and electron. We define average quark chemical potential by

$$\mu_q = \frac{\mu_u n_u + \mu_d n_d + \mu_s n_s}{n_u + n_d + n_s}. \quad (3.12)$$

The four independent chemical potentials are constrained by three conditions, there is only one independent chemical potential, we can free to choose μ_q as that one. Effective masses of quarks varying with μ_q are displayed in Fig. 3. We can see from Fig. 3 that the Nambu solutions keep constants at $\mu_q < 315$ MeV, and disappear thereafter, while the Wigner solution exists on the whole region of quark chemical potential. In principle, the physical solution has the maximum pressure, but the bag constant, namely the pressure between Nambu and Wigner solution in a vacuum, is often introduced as a parameter in the NJL-like model. We assume the chiral phase transition happens at the location of Nambu solution disappears, that is $\mu_q^c = 315$ MeV. The quark number densities varying

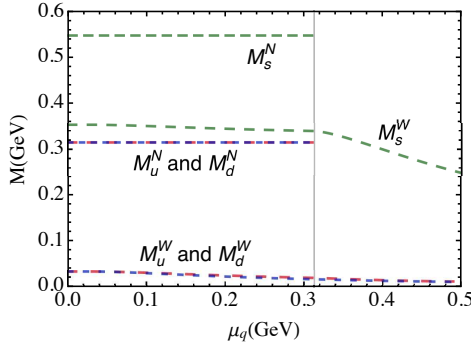


Figure 3. Effective masses of quarks for both Nambu and Wigner solutions, the superscript ‘N’ means Nambu solution, ‘W’ means Wigner solution.

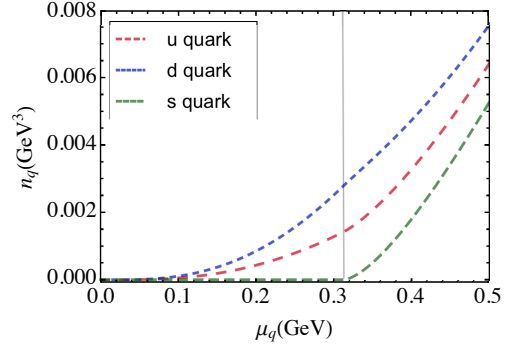


Figure 4. Quark number densities as functions of μ_q .

with μ_q are displayed in Fig. 4. The densities of u- and d-quark for the Nambu solution appear at 314.6 MeV and are very small compared to the densities in the Wigner solution. The densities suffer a discontinuity since the nature chooses Wigner solution at $\mu_q > \mu_q^c$. We can see that the s-quark appears very early because the quark condensates are smaller in the Wigner phase, which feedbacks to the effective interaction strength. The nature also choose the Wigner solution for s quark, its effective mass $M_s^W(\mu_q = 315\text{MeV}) = 339$ MeV is lower than its effective chemical potential $\mu_s^*(\mu_q = 315\text{MeV}) = 367$ MeV.

Based on our calculations, the densities of up and down quarks are very small, and the strange quark does not exist in the Nambu phase. After the chiral phase transition, nature favors the Wigner solution, all quarks have lower effective masses, densities suffer discontinuities. The strange quark appears simultaneously. The transfer of chemical potentials is illustrated in Fig. 5.

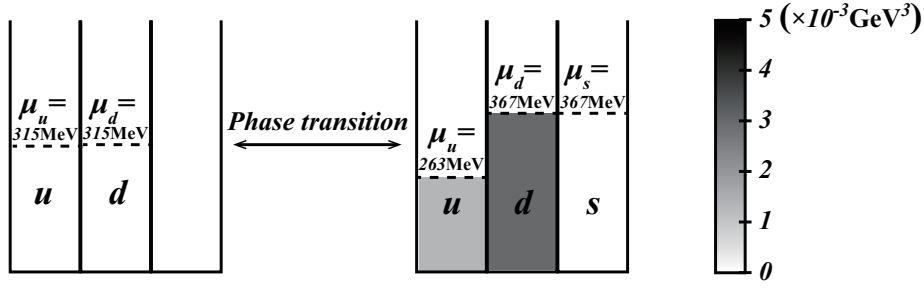


Figure 5. The schematic illustration of the change of chemical potentials and quark number densities in the chiral phase transition (The quark number densities are represented by darkness).

4 Application to strange quark stars

The EOS of cold and dense quark matter plays a significant role in studying the structure of compact stars. We plot the EOS in Fig. 6, which is based on the phase properties of dense quark matter in conditions of electric charge neutrality and β equilibrium. The pressure is calculated by [53]

$$P(\mu_q) = \int_0^{\mu_q} (n_u(\mu'_q) d\mu_u(\mu'_q) + n_d(\mu'_q) d\mu_d(\mu'_q) + n_s(\mu'_q) d\mu_s(\mu'_q) + n_e(\mu'_q) d\mu_e(\mu'_q)). \quad (4.1)$$

It has relation with energy density

$$\varepsilon(\mu_q) = -P(\mu_q) + \sum_i \mu_i(\mu_q) n_i(\mu_q). \quad (4.2)$$

In Fig. 6, we can see that the EOSs tend to coincident in the large pressure region, while they have little difference at low pressure. It implies the EOS is not too parameter-dependent in this model.

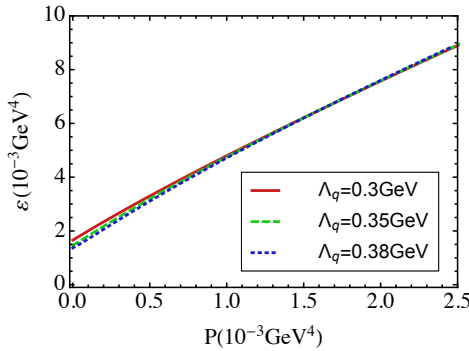


Figure 6. The quark scalar and pseudo scalar condensate varying with μ_I .

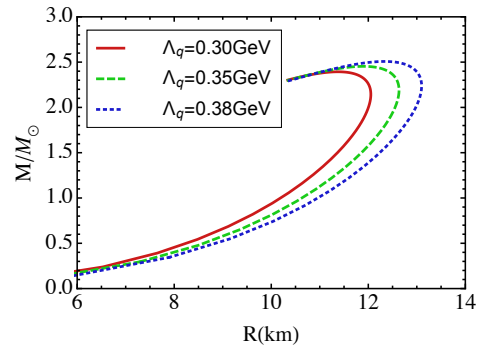


Figure 7. Mass-radius relation of strange quark stars.

The relation between mass and radius of compact stars is governed by Tolman-Oppenheimer-

Volkoff (TOV) equation,

$$\frac{dP(r)}{dr} = -\frac{G(\varepsilon + P)(M + 4\pi r^3 P)}{r(r - 2GM)}, \quad (4.3)$$

$$\frac{dM(r)}{dr} = 4\pi r^2 \varepsilon, \quad (4.4)$$

where the natural unit has used, $\hbar = 1 = c$. Take the EOS as input into Eqs. (4.3) and (4.4), one can solve the TOV equation numerically, the mass-radius relation is illustrated in Fig. 7. We can see that the curves are apparently separate from each other, which indicates that the mass-radius relations are very sensitive to the EOSs. When we take a look at the maximum mass of the strange quark star, they are $(2.39, 2.45, 2.51)M_\odot$ for $\Lambda_q = (0.30, 0.35, 0.38)$ GeV respectively. We find that the maximum mass is not sensitive to the parameter Λ_q .

5 Summary

We generalize the two flavor contact interaction model to the three-flavor case, the model parameters are fitted by pion and kaon observables. Analyzing the solution of quark DSE, there is only one solution, Nambu solution or chiral symmetry breaking solution, in a vacuum. Based on the ideas from Ref. [1, 2], we introduce a feedback term from quark condensates to coupling strength. The Wigner solution appears at some region of Λ_q . We mainly discuss $\Lambda_q \in (0.3, 0.381)$ GeV, since the Nambu and Wigner solution coexists and the largest mass equals the original one.

After fixing the model parameters, we study the chiral phase transition in the conditions of electric charge neutrality and β equilibrium. During the phase transition, all quark masses and number densities suffer discontinuities. The strange quark appears since nature favors the lower effective mass and $\mu_s^* > M_s$. At the phase transition point, the two phases coexist. The u-quark has smaller chemical potential in the chiral symmetry partially restoring phase, while d-quark has bigger value of chemical potential. Therefore, the system would need more energy to produce a d-quark than an s-quark if the density of the s-quark is very small.

EOSs of dense quark matter with neutrality is shown for three different Λ_q , they are almost coincident in the large pressure region, and have little difference at low pressure. Take EOSs as inputs to the TOV equations, the mass-radius relation for strange quark stars are drawn, which are very sensitive to the EOSs. The maximum mass of strange quark stars is not susceptible to the parameter Λ_q , its value reaches $2.39M_\odot$ or even $2.51M_\odot$.

Acknowledgments

This work is supported in part by the National Natural Science Foundation of China (under Grant No. 11905107), the National Natural Science Foundation of Jiangsu Province of China (under Grant No. BK20190721), Natural Science Foundation of the Jiangsu Higher Education Institutions of China (under Grant No. 19KJB140016), Nanjing University of

Posts and Telecommunications Science Foundation (under grant No. NY129032), Innovation Program of Jiangsu Province.

References

- [1] Y. Jiang, H. Gong, W.-m. Sun and H.-s. Zong, *Wigner solution of the quark gap equation at nonzero current quark mass and partial restoration of chiral symmetry at finite chemical potential*, *Phys. Rev. D* **85** (Feb, 2012) 034031.
- [2] Z.-f. Cui, C. Shi, Y.-h. Xia, Y. Jiang and H.-s. Zong, *The wigner solution of quark gap equation and chiral phase transition of qcd at finite temperature and nonzero chemical potential*, *The European Physical Journal C* **73** (2013) 1–8.
- [3] A. R. Bodmer, *Collapsed nuclei*, *Phys. Rev. D* **4** (Sep, 1971) 1601–1606.
- [4] E. Witten, *Cosmic separation of phases*, *Phys. Rev. D* **30** (Jul, 1984) 272–285.
- [5] M. G. Alford, K. Rajagopal, S. Reddy and A. W. Steiner, *Stability of strange star crusts and strangelets*, *Phys. Rev. D* **73** (Jun, 2006) 114016.
- [6] P. Jaikumar, S. Reddy and A. W. Steiner, *Strange star surface: A crust with nuggets*, *Phys. Rev. Lett.* **96** (Jan, 2006) 041101.
- [7] S. Chakrabarty, *Equation of state of strange quark matter and strange star*, *Phys. Rev. D* **43** (Jan, 1991) 627–630.
- [8] R. Tikekar and K. Jotania, *On relativistic models of strange stars*, *Pramana* **68** (2007) 397–406.
- [9] F. Rahaman, K. Chakraborty, P. Kuhfittig, G. Shit and M. Rahman, *A new deterministic model of strange stars*, *The European Physical Journal C* **74** (2014) 1–5.
- [10] M. Kalam, A. A. Usmani, F. Rahaman, S. M. Hossein, I. Karar and R. Sharma, *A relativistic model for strange quark star*, *International Journal of Theoretical Physics* **52** (2013) 3319–3328.
- [11] E. Zhou, A. Tsokaros, K. b. o. Uryū, R. Xu and M. Shibata, *Differentially rotating strange star in general relativity*, *Phys. Rev. D* **100** (Aug, 2019) 043015.
- [12] I. Bombaci, A. Drago, D. Logoteta, G. Pagliara and I. Vidaña, *Was gw190814 a black hole–strange quark star system?*, *Phys. Rev. Lett.* **126** (Apr, 2021) 162702.
- [13] G. Wiktorowicz, A. Drago, G. Pagliara and S. B. Popov, *Strange quark stars in binaries: formation rates, mergers, and explosive phenomena*, *The Astrophysical Journal* **846** (2017) 163.
- [14] W. Husain and A. W. Thomas, *Hybrid stars with hyperons and strange quark matter*, in *AIP Conference Proceedings*, vol. 2319, p. 080001, AIP Publishing LLC, 2021.
- [15] A. Kuerban, J.-J. Geng and Y.-F. Huang, *Gw emission from merging strange quark star-strange quark planet systems*, in *AIP Conference Proceedings*, vol. 2127, p. 020027, AIP Publishing LLC, 2019.
- [16] P. K. Srivastava, S. K. Tiwari and C. P. Singh, *Qcd critical point in a quasiparticle model*, *Phys. Rev. D* **82** (Jul, 2010) 014023.
- [17] S. Plumari, W. M. Alberico, V. Greco and C. Ratti, *Recent thermodynamic results from lattice qcd analyzed within a quasiparticle model*, *Phys. Rev. D* **84** (Nov, 2011) 094004.

- [18] K. K. Szabó and A. I. Tóth, *Quasiparticle description of the qcd plasma, comparison with lattice results at finite t and μ* , *Journal of High Energy Physics* **2003** (2003) 008.
- [19] C. Sasaki and K. Redlich, *Bulk viscosity in quasiparticle models*, *Phys. Rev. C* **79** (May, 2009) 055207.
- [20] R. A. Schneider and W. Weise, *Quasiparticle description of lattice qcd thermodynamics*, *Phys. Rev. C* **64** (Oct, 2001) 055201.
- [21] M. A. Thaler, R. A. Schneider and W. Weise, *Quasiparticle description of hot qcd at finite quark chemical potential*, *Phys. Rev. C* **69** (Mar, 2004) 035210.
- [22] A. Peshier, B. Kämpfer and G. Soff, *Equation of state of deconfined matter at finite chemical potential in a quasiparticle description*, *Phys. Rev. C* **61** (Mar, 2000) 045203.
- [23] B.-J. Schaefer and J. Wambach, *The phase diagram of the quark–meson model*, *Nuclear Physics A* **757** (2005) 479–492.
- [24] H. Ueda, T. Z. Nakano, A. Ohnishi, M. Ruggieri and K. Sumiyoshi, *Qcd phase diagram at finite baryon and isospin chemical potentials in the polyakov loop extended quark meson model with vector interaction*, *Phys. Rev. D* **88** (Oct, 2013) 074006.
- [25] B.-J. Schaefer, J. M. Pawłowski and J. Wambach, *Phase structure of the polyakov-quark-meson model*, *Phys. Rev. D* **76** (Oct, 2007) 074023.
- [26] K. Kamikado, N. Strodthoff, L. von Smekal and J. Wambach, *Fluctuations in the quark-meson model for qcd with isospin chemical potential*, *Physics Letters B* **718** (2013) 1044–1053.
- [27] R.-A. Tripolt, B.-J. Schaefer, L. von Smekal and J. Wambach, *Low-temperature behavior of the quark-meson model*, *Phys. Rev. D* **97** (Feb, 2018) 034022.
- [28] N. Tetradis, *The quark–meson model and the phase diagram of two-flavour qcd*, *Nuclear Physics A* **726** (2003) 93–119.
- [29] G. Endrődi and G. Markó, *Magnetized baryons and the qcd phase diagram: Njl model meets the lattice*, *Journal of High Energy Physics* **2019** (2019) 1–17.
- [30] M. Wakayama and A. Hosaka, *Search of qcd phase transition points in the canonical approach of the njl model*, *Physics Letters B* **795** (2019) 548–553.
- [31] Y. Lu, Y.-L. Du, Z.-F. Cui and H.-S. Zong, *Critical behaviors near the (tri-) critical end point of qcd within the njl model*, *The European Physical Journal C* **75** (2015) 1–7.
- [32] T. Khunjua, K. Klimenko and R. N. Zhokhov, *Qcd phase diagram with chiral imbalance in njl model: duality and lattice qcd results*, in *Journal of Physics: Conference Series*, vol. 1390, p. 012015, IOP Publishing, 2019.
- [33] L. Yu, H. Liu and M. Huang, *Effect of the chiral chemical potential on the chiral phase transition in the njl model with different regularization schemes*, *Phys. Rev. D* **94** (Jul, 2016) 014026.
- [34] Z.-f. Cui, C. Shi, W.-m. Sun, Y.-l. Wang and H.-s. Zong, *The wigner solution and qcd phase transitions in a modified pnjl model*, *The European Physical Journal C* **74** (2014) 1–9.
- [35] X. Wang, M. Wei, Z. Li and M. Huang, *Quark matter under rotation in the njl model with vector interaction*, *Phys. Rev. D* **99** (Jan, 2019) 016018.
- [36] F. Gao and J. M. Pawłowski, *Qcd phase structure from functional methods*, *Phys. Rev. D* **102** (Aug, 2020) 034027.

- [37] C. Shi, Y.-l. Wang, Y. Jiang, Z.-f. Cui and H.-S. Zong, *Locate qcd critical end point in a continuum model study*, *Journal of High Energy Physics* **2014** (2014) 1–10.
- [38] Y. Jiang, H. Chen, W.-M. Sun and H.-S. Zong, *Chiral phase transition of qcd at finite chemical potential*, *Journal of High Energy Physics* **2013** (2013) 1–12.
- [39] C. S. Fischer, J. Luecker and C. A. Welzbacher, *Phase structure of three and four flavor qcd*, *Phys. Rev. D* **90** (Aug, 2014) 034022.
- [40] C. S. Fischer, J. Luecker and J. A. Mueller, *Chiral and deconfinement phase transitions of two-flavour qcd at finite temperature and chemical potential*, *Physics Letters B* **702** (2011) 438–441.
- [41] C. S. Fischer, J. Luecker and C. A. Welzbacher, *Locating the critical end point of qcd*, *Nuclear Physics A* **931** (2014) 774–779.
- [42] C. Shi, Y.-L. Du, S.-S. Xu, X.-J. Liu and H.-S. Zong, *Continuum study of the qcd phase diagram through an ope-modified gluon propagator*, *Phys. Rev. D* **93** (Feb, 2016) 036006.
- [43] F. Gao and Y.-x. Liu, *Interface effect in qcd phase transitions via dyson-schwinger equation approach*, *Phys. Rev. D* **94** (Nov, 2016) 094030.
- [44] W.-j. Fu, J. M. Pawłowski and F. Rennecke, *Qcd phase structure at finite temperature and density*, *Phys. Rev. D* **101** (Mar, 2020) 054032.
- [45] C. Shi, X.-T. He, W.-B. Jia, Q.-W. Wang, S.-S. Xu and H.-S. Zong, *Chiral transition and the chiral charge density of the hot and dense qcd matter.*, *Journal of High Energy Physics* **2020** (2020) 1–18.
- [46] F. Gao and J. M. Pawłowski, *Chiral phase structure and critical end point in qcd*, *Physics Letters B* **820** (2021) 136584.
- [47] C. S. Fischer, J. Luecker and J. M. Pawłowski, *Phase structure of qcd for heavy quarks*, *Phys. Rev. D* **91** (Jan, 2015) 014024.
- [48] G. Eichmann, C. S. Fischer and C. A. Welzbacher, *Baryon effects on the location of qcd’s critical end point*, *Phys. Rev. D* **93** (Feb, 2016) 034013.
- [49] L. Chang, Y.-X. Liu, M. S. Bhagwat, C. D. Roberts and S. V. Wright, *Dynamical chiral symmetry breaking and a critical mass*, *Phys. Rev. C* **75** (Jan, 2007) 015201.
- [50] S. P. Klevansky, *The nambu—jona-lasinio model of quantum chromodynamics*, *Rev. Mod. Phys.* **64** (Jul, 1992) 649–708.
- [51] PARTICLE DATA GROUP collaboration, P. Zyla et al., *Review of Particle Physics*, *PTEP* **2020** (2020) 083C01.
- [52] F. Burger, V. Lubicz, M. Müller-Preussker, S. Simula and C. Urbach, *Quark mass and chiral condensate from the wilson twisted mass lattice quark propagator*, *Phys. Rev. D* **87** (Feb, 2013) 034514.
- [53] H.-S. Zong and W.-M. Sun, *A model study of the equation of state of qcd*, *International Journal of Modern Physics A* **23** (2008) 3591–3612.